

## Electronic Supplementary Information

### **Enhanced Photoelectric Performance in Cu-Bi Double Halide Perovskite Single Crystals**

Shuang Wu, Wen-Guang Li, Yu-Hua Huang, Xu-Dong Wang,\* and Dai-Bin Kuang

Key Laboratory of Bioinorganic and Synthetic Chemistry of Ministry of Education,  
LIFM, GBRCE for Functional Molecular Engineering, School of Chemistry, IGCME,  
Sun Yat-Sen University, Guangzhou 510275, China

E-mail: wangxd26@mail.sysu.edu.cn.

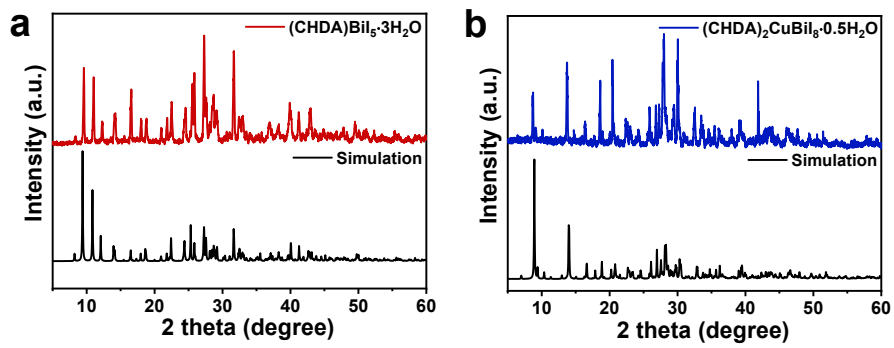


**Fig. S1** Powder XRD patterns of a)  $(\text{CHDA})\text{BiI}_5 \cdot 3\text{H}_2\text{O}$  and b)  $(\text{CHDA})_2\text{CuBiI}_8 \cdot 0.5\text{H}_2\text{O}$  powders, respectively.

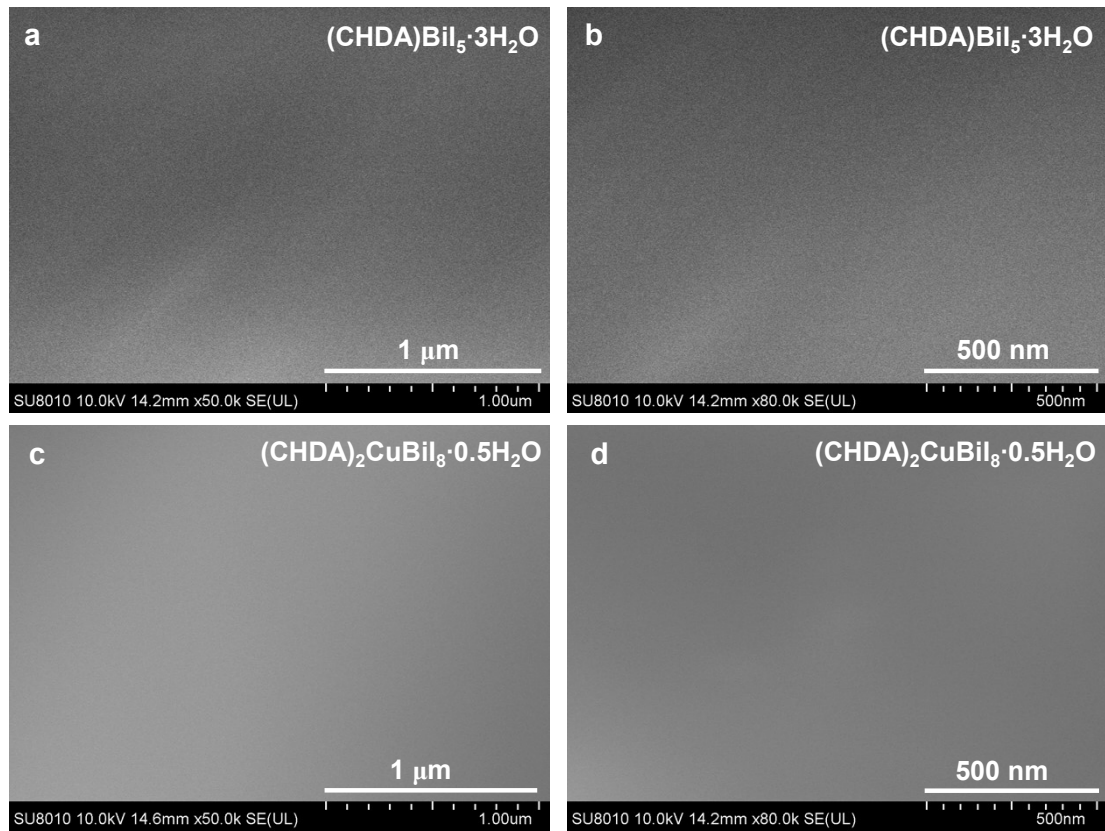


**Fig. S2** SEM images of a, b)  $(\text{CHDA})\text{BiI}_5 \cdot 3\text{H}_2\text{O}$  and c, d)  $(\text{CHDA})_2\text{CuBiI}_8 \cdot 0.5\text{H}_2\text{O}$  SCs, respectively.

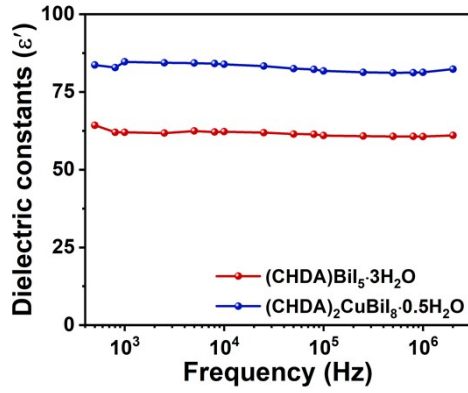


**Fig. S3** The frequency dependent dielectric curves of the (CHDA)BiI<sub>5</sub>·3H<sub>2</sub>O and (CHDA)<sub>2</sub>CuBiI<sub>8</sub>·0.5H<sub>2</sub>O SCs. It should be pointed out that the devices used to measure the relative dielectric constant adopts a parallel structure, as same as that in subsequent photodetectors. The calculation method is proposed in the references reported, previously.<sup>1-3</sup>

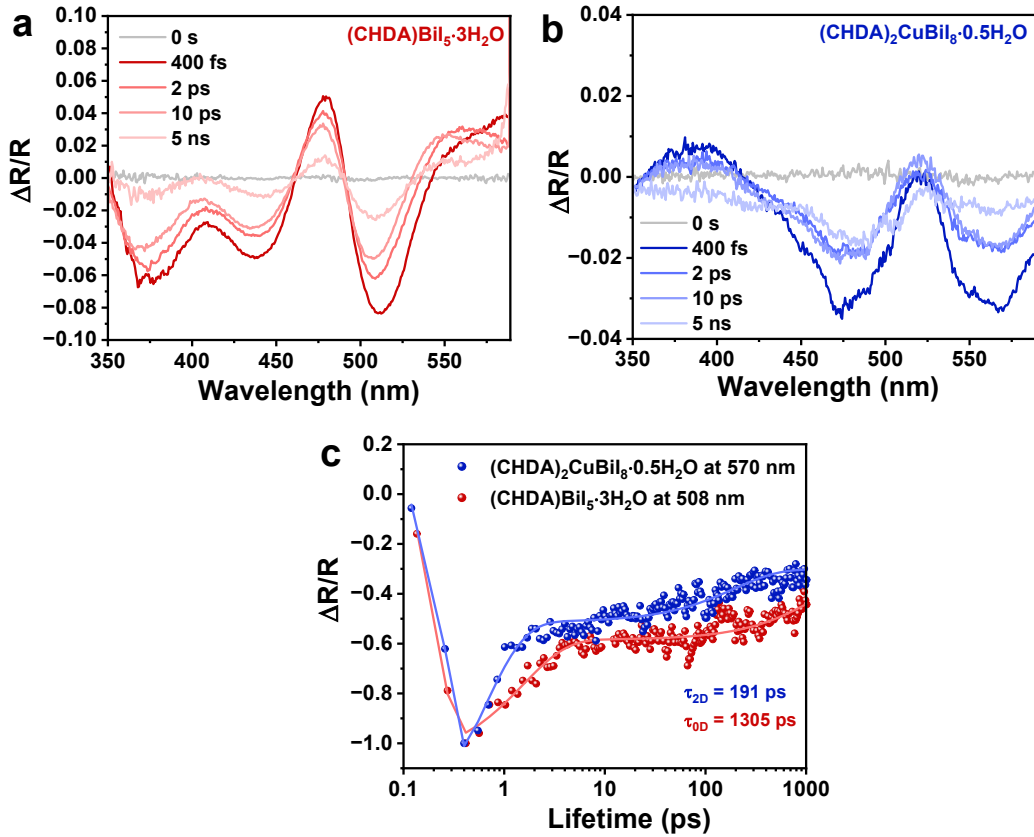


**Fig. S4** The TR spectra of a) the (CHDA)BiI<sub>5</sub>·3H<sub>2</sub>O and b) (CHDA)<sub>2</sub>CuBiI<sub>8</sub>·0.5H<sub>2</sub>O SCs. c) TR kinetic fit of (CHDA)BiI<sub>5</sub>·3H<sub>2</sub>O and (CHDA)<sub>2</sub>CuBiI<sub>8</sub>·0.5H<sub>2</sub>O SCs recorded at 508 and 570 nm, respectively.

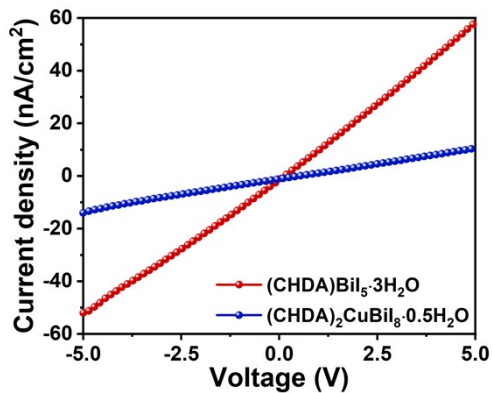


**Fig. S5**  $i$ - $v$  curves of the  $(\text{CHDA})\text{BiI}_5\cdot 3\text{H}_2\text{O}$  and  $(\text{CHDA})_2\text{CuBiI}_8\cdot 0.5\text{H}_2\text{O}$  SC photodetectors measured in the dark.

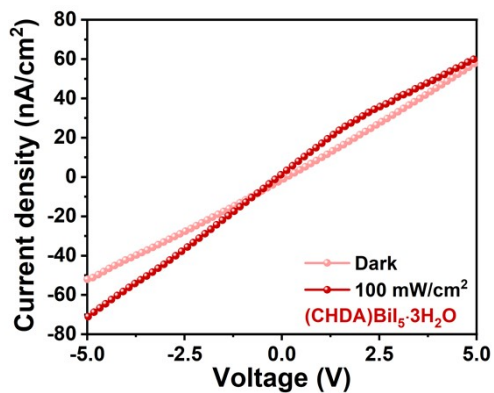


**Fig. S6**  $i$ - $v$  curves of the  $(\text{CHDA})\text{BiI}_5\cdot 3\text{H}_2\text{O}$  SC photodetector measured in the dark and under white LED illumination with  $100 \text{ mW cm}^{-2}$ .

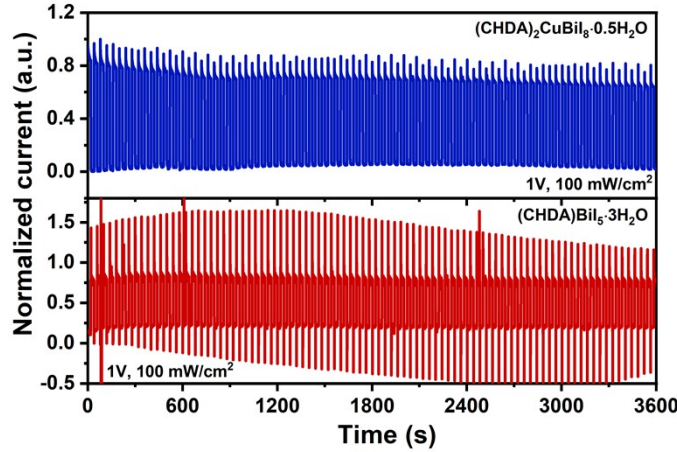


**Fig. S7** The on/off switching cycles of the photocurrent of the unencapsulated  $(\text{CHDA})\text{BiI}_5 \cdot 3\text{H}_2\text{O}$  and  $(\text{CHDA})_2\text{CuBiI}_8 \cdot 0.5\text{H}_2\text{O}$  SC photodetectors, during 60 min continuous operation under chopped white LED illumination (20 s on, 20 s off) with  $100 \text{ mW cm}^{-2}$  at 1 V.

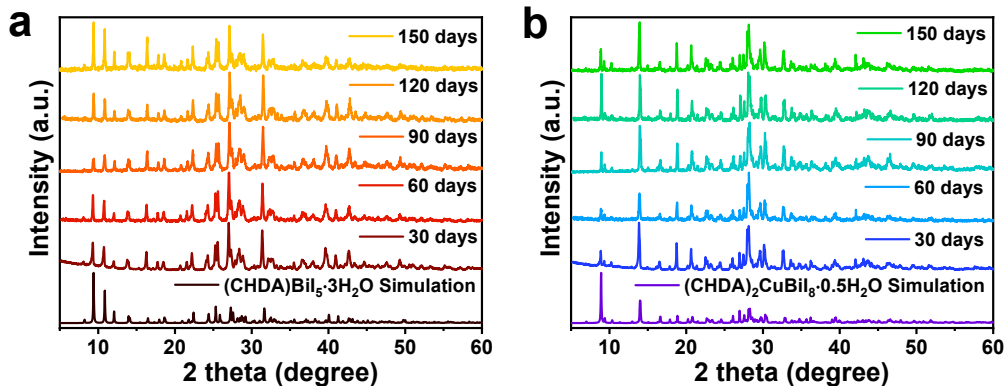


**Fig. S8** XRD stability tests of a)  $(\text{CHDA})\text{BiI}_5 \cdot 3\text{H}_2\text{O}$  and b)  $(\text{CHDA})_2\text{CuBiI}_8 \cdot 0.5\text{H}_2\text{O}$  powders, stored in ambient air at a humidity of  $\sim 70\%$ RH.

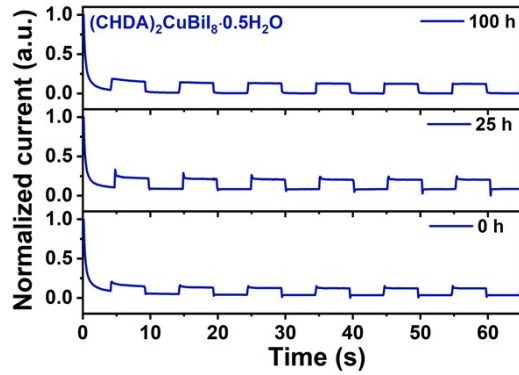


**Fig. S9** Photoresponse of the unencapsulated  $(\text{CHDA})_2\text{CuBiI}_8 \cdot 0.5\text{H}_2\text{O}$  SC device was measured for 100 h of exposure time in ambient air with humidity at  $\sim 70\%$  RH.

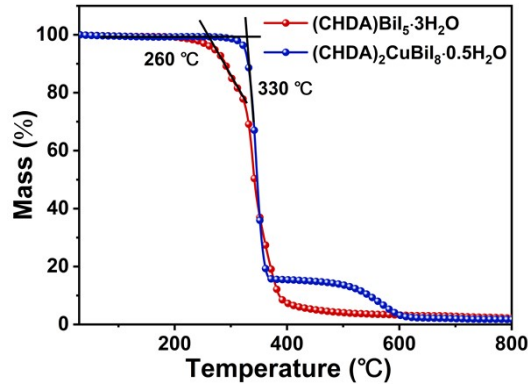


**Fig. S10** TGA curves of  $(\text{CHDA})\text{BiI}_5 \cdot 3\text{H}_2\text{O}$  and  $(\text{CHDA})_2\text{CuBiI}_8 \cdot 0.5\text{H}_2\text{O}$ .

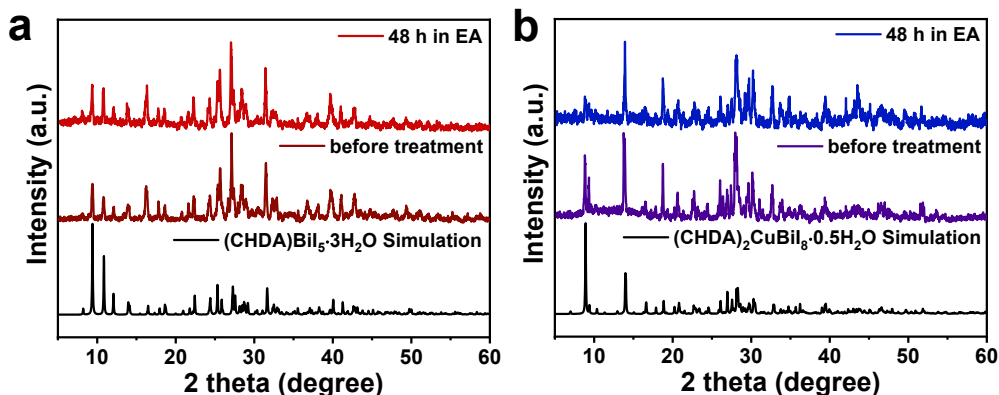


**Fig. S11** a, b) the corresponding XRD patterns of two perovskite powders before and after soaking in EA.

**Table S1.** Concentration table of each raw materials in the synthesis process.

<b>Product</b>	<b>CHDA</b>	<b>BiI<sub>3</sub></b>	<b>CuI</b>
(CHDA)BiI <sub>5</sub> ·3H <sub>2</sub> O	0.06 mol L <sup>-1</sup>	0.06 mol L <sup>-1</sup>	--
(CHDA) <sub>2</sub> CuBiI <sub>8</sub> ·0.5H <sub>2</sub> O	0.18 mol L <sup>-1</sup>	0.06 mol L <sup>-1</sup>	0.12 mol L <sup>-1</sup>

**Table S2.** Crystallographic data of the (CHDA)BiI<sub>5</sub>·3H<sub>2</sub>O and (CHDA)<sub>2</sub>CuBiI<sub>8</sub>·0.5H<sub>2</sub>O.

<b>Empirical formula</b>	<b>C<sub>6</sub>H<sub>16</sub>N<sub>2</sub>BiI<sub>5</sub>·3H<sub>2</sub>O</b>	<b>(C<sub>6</sub>H<sub>16</sub>N<sub>2</sub>)<sub>2</sub>CuBiI<sub>8</sub>·0.5H<sub>2</sub>O</b>
Formula weight (g/mol)	1013.73	1529.14
Crystal system	monoclinic	monoclinic
Space group	P2 <sub>1</sub> /c	P2 <sub>1</sub> /n
a/Å	11.5808(8)	17.062(6)
b/Å	12.5195(8)	19.825(7)
c/Å	15.3418(9)	18.808(7)
α/°	90	90
β/°	111.928(3)	90.297(5)
γ/°	90	90
Volume/Å <sup>3</sup>	2063.4(2)	6362(4)
Z	4	8
ρ <sub>calc</sub> (g/cm <sup>3</sup> )	3.263	3.193
Goodness-of-fit on F <sup>2</sup>	1.056	1.026

## References

- 1 H. N. Al-Shareef, D. Dimos, M. V. Raymond, R.W. Schwartz, C. H. Mueller, *J. Electroceram.* **1997**, *1*, 145-153.
- 2 N. J. Kidne, A. Meier, Z. J. Homrighaus, B. W. Wessels, T. O. Mason, E. J. Garboczi, *Thin Solid Films.* **2007**, *515*, 4588-4595.
- 3 H. Liu, J. Zhu, D. Xiao, X. Gong, J. Liang, X. Li, X. Zhu, *Appl. Phys. Lett.* **2007**, *91*, 182907.